The effect of hydrogen on the electronic structure and phase stability of iron-based alloys doped with chromium and nickel

1998 J. Phys.: Condens. Matter 10 6987

(http://iopscience.iop.org/0953-8984/10/31/014)

J. Phys.: Condens. Matter **10** (1998) 6987–6994. Printed in the UK PII: S0953-8984(98)91414-X

The effect of hydrogen on the electronic structure and phase stability of iron-based alloys doped with chromium and nickel

A G Vakhney†§, A N Yaresko†, V N Antonov†, V V Nemoshkalenko†, V G Gavriljuk†, A V Tarasenko† and I Smurov‡

† Institute of Metal Physics, 36 Vernadsky Boulevard, 252142 Kiev, Ukraine
‡ Ecole Nationale d'Engenieurs de Saint-Etienne, 58 Rue Jean Parot, 42023 Saint-Etienne Cédex 2, France

Received 5 February 1998

Abstract. The electronic structures and cohesive properties of the hydrogenated face-centred cubic (FCC) and hexagonal close-packed (HCP) phases of the CrNiFe alloy have been studied using the first-principles linear muffin-tin orbital method combined with an x-ray diffraction study. The cohesion energy of these crystalline phases is calculated as a function of the Wigner–Seitz radius. The predicted structure is in agreement with that observed experimentally and the calculated equilibrium lattice parameters are in good agreement with the experimental values. The electronic structure is used to determine the relative stability of different structures. It is shown that the nature of the FCC $\rightarrow$ HCP transformation in CrNiFe alloy is due to the weakening of the interatomic bond.

1. Introduction

Hydrogen, introduced into engineering materials, causes brittleness, whose nature still remains a controversial issue. Among the hypotheses advanced as possible explanations for hydrogen embrittlement are the following three suggestions:

(i) weakening of the interatomic bond,
(ii) hydrogen-enhanced localized plasticity and
(iii) formation of brittle pseudohydrides—this suggestion is still under active discussion (see, for example, [1]).

Hydrogenation of certain FCC iron-based alloys which constitute an array of stainless austenitic steels causes the phase transformations FCC(γ)$\rightarrow$BCC(α_{H}) and FCC(γ)$\rightarrow$HCP(ε_{H}), the hydrogen-induced phases usually being considered as pseudo-hydrides (see, e.g., [2–5]). In the case of the so-called stable austenitic steels which have not undergone phase transformations during cooling to 4 K, hydrogen does not induce the α_{H}-martensite and the only hydrogen-induced phase is ε_{H} [2–4]. It is generally suggested that the role of hydrogen amounts to the creation of a particular stress state (see, e.g., [5, 6]), i.e., in fact, the ε_{H}-phase is a stress-induced ε-martensite and the role of the stresses caused by hydrogen in the FCC–HCP transformation is decisive. On the other hand, on account of the high hydrogen concentration in austenitic steels achieved due to the cathodic charging

§ Author to whom any correspondence should be addressed; e-mail: vakh@d24.imp.kiev.ua.

0953-8984/98/316987+08$19.50

(about 35 at.%; see [7–9]), one can expect a striking effect of hydrogen on the electronic structure and, as a result, on the thermodynamical stability of the FCC iron-based alloys.

This approach is supported by an x-ray study of the cathodically charged dual FCC+HCP (Fe+21% of Mn) solid solution [10], which has revealed a selective absorption of hydrogen by the HCP phase while the FCC austenite absorbs only a small quantity of hydrogen. The high hydrogen-gas-pressure hydrogenation which, in contrast to the cathodic charging, provides a homogeneous hydrogen saturation and excludes the possibility of the creation of significant stresses, has also shown that hydrogen in the Fe + 22% Mn alloy extends the temperature range of the stability of the HCP phase [11].

The aim of this study is to carry out an *ab initio* calculation of the effect of hydrogen on the electronic structure and the phase stability of FeCrNi alloy combined with an x-ray diffraction study of the transformations caused by hydrogen in stable austenitic steel.

Table 1. Chemical composition, wt.%.

Alloy	C	Cr	Ni	Mn	Si	S	P	Fe
CrNi 25 20	0.01	25.2	20.2	0.5	0.01	0.002	0.007	54.1

2. Experimental technique

CrNi 25 20 steel, of chemical composition close to that of AISI 310 (see table 1), was used for the x-ray studies. Plates about 0.5 mm in thickness were prepared after rolling and final solution treatment at 1150 °C followed by water quenching and etching.

Hydrogen charging was performed in 1N $H_2S0_4 + 0.25$ g l^{-1} $NaAsO_2$ solution at the current density of 50 mA cm^{-2}. After charging, the samples were stored in liquid nitrogen and then installed in a cryostat at 120 K and cooled to 25 K.

X-ray diffraction patterns were obtained at 40 and 100 K using a piece of equipment constructed from a tube with Co Kα radiation, a bent SiO_2 monochromator at the primary beam, the curved position-sensitive detector INEL CPS 120 and a closed-cycle cryo-refrigerator.

3. Experimental results

The fragments of the x-ray diffraction patterns of the CrNi 25 20 steel as solution treated (1), cold rolled to a reduction in thickness of 90% (2) and hydrogen charged (3) are shown in figure 1. The measurements of the as-quenched samples were performed at 40 K, while the cold-rolled and the hydrogen-charged samples were treated at 100 K. It is clearly seen that plastic deformation does not cause a FCC $\rightarrow$ HCP transformation even when it is combined with substantial cooling. At the same time, hydrogen has induced the ε_H-phase, which is not entirely consistent with the idea of a decisive role of stresses in transformations caused by hydrogen. The reflections of the ε_H-phase and those of the austenite remaining (γ_H) are shifted to smaller angles from the positions for the hydrogen-free phases, which corresponds to a lattice dilatation of about 5%. An evaluation of the hydrogen content according to the data from [7] gives a H/Me ratio of about 0.6 for both phases. This means that the transformation occurred after the FCC phase had absorbed some critical content of hydrogen, in contrast to the case in studies of duplex FCC+HCP steel [10], where hydrogen charging led to selective hydrogen absorption by the HCP phase.

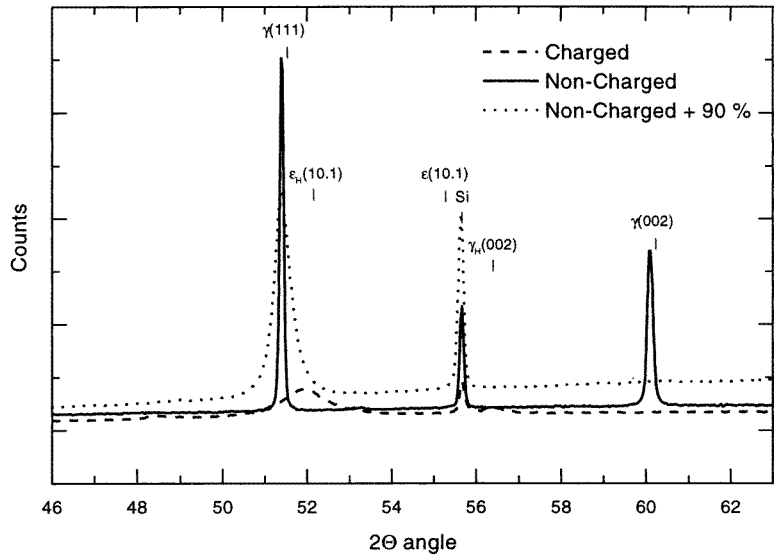

Figure 1. A fragment of the diffraction pattern of CrNi 25 20 steel after solution treatment at 1150 °C (1), solution treatment and cold rolling to a reduction in thickness of 90% (2) and solution treatment and hydrogen charging (3). Temperatures of the measurements: 40 K for (1) and 100 K for (2) and (3). The positions of the reflections are shown for ε (expected) and γ in the uncharged states, and ε_{H} and γ_{H} in the charged states.

4. Computational details

The present band-structure calculations were carried out using the self-consistent scalar-relativistic LMTO method in the atomic-sphere approximation (ASA) [12] with combined correction terms included. Exchange and correlation contributions to both atomic and crystal potentials were included through the density-functional description within the LSDA given by von Barth and Hedin [13]. Relativistic effects were included except for the spin–orbital coupling for valence electrons. The $\boldsymbol{k}$-integrated functions have been evaluated by the improved tetrahedron method [14] on a grid of 196 $\boldsymbol{k}$-points and 144 $\boldsymbol{k}$-points in the irreducible wedge of the Brillouin zone for the γ-phase and the ε-phase, respectively. Spherical harmonics with l up to 2 and 0 were included in the decomposition of the wavefunctions in the metal and the hydrogen atomic spheres, respectively.

The cohesive properties of the alloy were studied using the following definition of the cohesion energy per unit cell:

$$E_{coh} = E_{\mathrm{total}} - \sum E_i \tag{1}$$

where E_{total} is the total energy of the compound and $\sum E_i$ is the sum of the total energies of the constituent atoms [15].

5. Theoretical results

The total-energy calculations were performed for the γ- and ε-phases of $CrNiFe_2H_x$ alloy, where $x = 0, 2, 4$. To calculate the electronic band structures of the γ- and ε-phases, we used face-centred tetragonal ($P4/mmm$ space group) and hexagonal close-packed ($P\bar{6}m2$

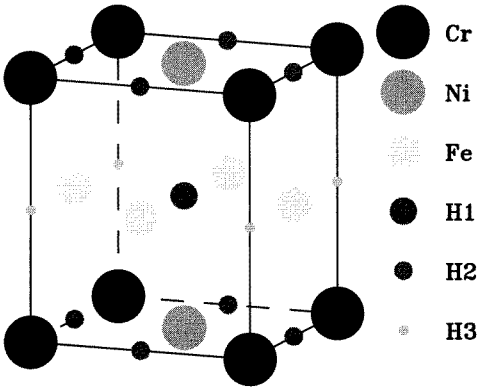

Figure 2. The unit cell of the γ-phase.

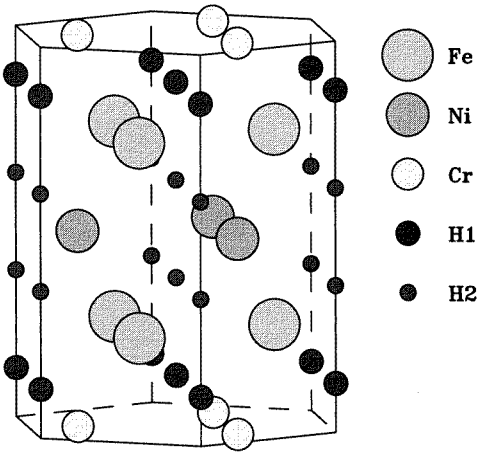

Figure 3. The unit cell of the ε-phase.

space group) crystal structures, respectively (see figures 2 and 3). Hydrogen atoms were placed in the interstitial octahedral holes of the unit cells of the γ- and ε-phases, indicated by the labels H1, H2 and H3. For $x = 2$, hydrogen atoms were placed at the H2 positions for the γ-phase and H1 positions for the ε-phase, as it was found that such an arrangement minimizes the total energy of the phase.

The cohesion energy versus the average Wigner–Seitz radius curves calculated for the γ- and ε-phases for different hydrogen contents are shown in figure 4. One can notice that without hydrogen added the γ-phase is more stable than the ε-phase.

For the $CrNiFe_2H_2$ compound a competition between the two phases is observed: the cohesion energies of the γ- and ε-phases are very close and reach their minima at values of the Wigner–Seitz radius that are almost the same. Thus, we can conclude that the $\gamma \rightarrow \varepsilon$-phase transition starts when about 2 hydrogen atoms per formula unit are absorbed by the alloy.

The situation changes when four hydrogen atoms are added. Then, the γ_H-phase is less stable than the ε_H-phase. The equilibrium values of the lattice parameter, determined as the positions of the minima of the corresponding cohesion energy curves, are given in

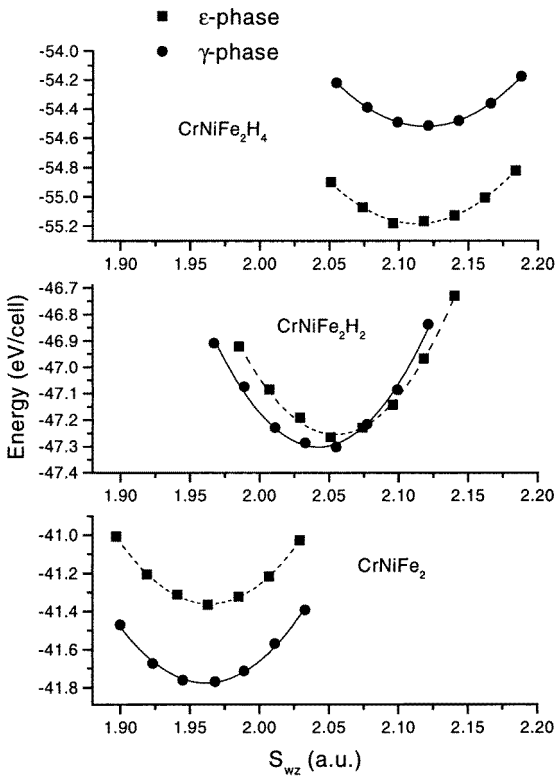

Figure 4. The cohesion energies of the γ- and ε-phases as functions of the Wigner–Seitz radius.

Table 2. Calculated equilibrium values of the lattice parameters for the γ- and ε-phases a_{equ}, compared with the experimental values a_{exp} (Å).

Phase	Alloy	a_{equ}	a_{exp}
γ	$CrNiFe_2$	3.350	3.58
	$CrNiFe_2H_2$	3.486	—
	$CrNiFe_2H_4$	3.619	3.76
ε	$CrNiFe_2$	2.370	2.53
	$CrNiFe_2H_2$	2.481	—
	$CrNiFe_2H_4$	2.550	2.66

table 2. The lattice dilatation for both γ- and ε-phases is about 8%, which agrees well with the experimental value of 5%. The equilibrium values of the lattice parameter are, also, in good agreement with experimental data [5]. Some difference may be explained by the presence of the admixtures of C, Si, S, P and quite a large amount of Mn in the experimental samples, which were not taken into account in the present calculations.

The total densities of states (DOS) for the γ- and ε-phases calculated at the equilibrium values of the lattice parameter are shown in figure 5. The valence bands of both the γ- and ε-phases of $CrNiFe_2H_x$ with $x = 0$ are formed mainly by Cr, Ni and Fe d states with

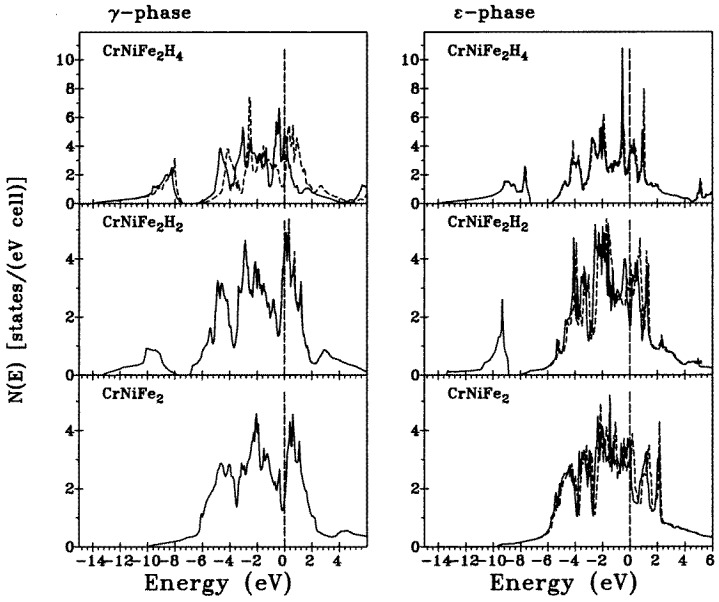

Figure 5. The total DOS of the γ- and ε-phases (states eV^{-1}/cell) (solid line: spin up; broken line: spin down).

some admixture of s states at the bottom of the valence band. For hydrogen-containing alloys, an additional peak appears at the bottom of the valence band, which is formed by H s states strongly hybridized with s and d states of transition metals. The width of this peak increases as the hydrogen content in the alloy becomes larger.

Table 3. The densities of states at the Fermi level $N(E_F)$ (states eV^{-1}/cell) for γ- and ε-$CrNiFe_2H_x$ calculated at the equilibrium values of the lattice parameter.

Phase	Alloy	$N(E_F)$
γ	$CrNiFe_2$	3.33
	$CrNiFe_2H_2$	8.80
	$CrNiFe_2H_4$	11.68
ε	$CrNiFe_2$	10.47
	$CrNiFe_2H_2$	5.45
	$CrNiFe_2H_4$	6.80

A conclusion concerning the relative stability of the phases is often derived from a comparison of the values of their densities of states at the Fermi level $N(E_F)$—that is, the lower $N(E_F)$, the more stable the corresponding phase. To establish whether this criterion is valid in the case of the γ- and ε-phases of $CrNiFe_2H_x$ alloy, we present in table 3 the calculated values of $N(E_F)$. When no hydrogen is added, $N(E_F)$ for the γ-phase is significantly lower than that for the ε-phase, which, in accordance with the results of the total-energy calculations and the experimental data, indicates that the former is more stable. Due to an increase of the number of valence electrons caused by hydrogen charging, the Fermi energies of both the γ- and ε-phases increase; however, the change in the position of

the Fermi level results in opposite changes in $N(E_F)$. The Fermi level for the γ-phase shifts to the region of high density of states, whereas E_F for the ε-phase shifts to a minimum of the DOS (see figure 5). Hence, the changes of $N(E_F)$ confirm the conclusion, derived from the comparison of the cohesion energies, that during hydrogen charging the γ_{H}-phase becomes less stable as compared to ε_{H}-phase.

Table 4. The magnetic moments of Cr, M_{Cr}, of Ni, M_{Ni}, of Fe M_{Fe}, and the average moment per 3d atom, M_{ave} (μ_B).

Phase	Alloy	M_{Cr}	M_{Ni}	M_{Fe}	M_{ave}
γ	$CrNiFe_2$	0.00	0.00	0.00	0.00
	$CrNiFe_2H_2$	−0.41	0.20	0.90	0.40
	$CrNiFe_2H_4$	1.25	0.34	1.11	1.20
ε	$CrNiFe_2$	−0.10	0.25	0.32	0.20
	$CrNiFe_2H_2$	−0.13	0.56	0.21	0.21
	$CrNiFe_2H_4$	0.00	0.00	0.00	0.00

It is well known that a high density of states at E_F may lead not only to structural instability but also to magnetic instability. Therefore, for equilibrium values of the lattice constant, spin-polarized calculations of the electronic structure of $CrNiFe_2H_x$ were performed. Local Cr, Fe and Ni magnetic moments and average magnetic moments per 3d atom calculated for the γ- and ε-phases are listed in table 4. In accordance with the fact that austenite is not a ferromagnetic phase, no magnetic solution was found for γ-$CrNiFe_2$. As a result of the hydrogen charging, the γ-phase becomes magnetic. The average magnetic moment increases proportionally to the hydrogen content and reaches the value of 1.2 μ_B/atom for $CrNiFe_2H_4$. The average magnetic moment of the ε-phase increases slightly when two hydrogen atoms are added, but for $CrNiFe_2H_4$ a non-magnetic solution was obtained. The decrease of the magnetic moment when going from $CrNiFe_2H_2$ to $CrNiFe_2H_4$ is confirmed by the experimental data on the magnetization [4].

As for the relative stability of the γ- and ε-phases, accounting for the effects of spin polarization does not affect the conclusions obtained from the non-spin-polarized total-energy calculations. It was found that the gain in the total energy due to magnetic ordering is much smaller than the difference between the total energies of the γ- and ε-phases with the same hydrogen content.

6. Conclusions

The FCC $\rightarrow$ HCP phase transformation in $CrNiFe_2H_x$ alloy is due to the change in the electronic structure. During the hydrogen charging, the DOS at E_F increases, which causes a weakening of the interatomic bonds and, consequently, an instability of the austenite and a phase transformation.

Acknowledgments

This work was accomplished partly within the framework of the INCO–Copernicus Project 960080 ‘Virtual Technological Experiment in Welding’ and has been supported by the CRDF project UP1-328.

References

[1] Birnbaum H K 1990 *Hydrogen Effects on Material Behaviour* ed N R Moody and A W Thompson (Warrendale, PA: AIME) p 639
[2] Kamachi K 1978 *Trans. ISIJ* **18** 485
[3] Mathias H, Katz Y and Nadiv S 1978 *Met. Sci.* **35** 2329
[4] Narita N, Altstetter C J and Birnbaum H K 1982 *Metall. Trans.* A **13** 129
[5] Szummer A and Janko A 1979 *Corrosion* **35** 461
[6] Tähtinen S, Nenonen P and Hänninen H 1986 *Scr. Metall.* **20** 153
[7] Baranowski B, Majchrzak S and Flanagan T B 1971 *J. Phys. F: Met. Phys.* **1** 258
[8] Farrel K and Lewis M B 1981 *Scr. Metall.* **15** 661
[9] Ulmer D G and Altstetter C J 1993 *Acta Metall. Mater.* **41** 2235
[10] Aikawa T, Nishino Y and Asano S 1993 *Scr. Metall.* **29** 135
[11] Ponyatowsky E G, Antonov V E and Belash I T 1978 *Fiz. Met. Metalloved.* **46** 170
[12] Andersen O K 1975 *Phys. Rev.* B **12** 3060
[13] von Barth U and Hedin L 1972 *J. Phys. C: Solid State Phys.* **5** 1629
[14] Blöchl P E, Jepsen O and Andersen O K 1994 *Phys. Rev.* B **49** 16 223
[15] Liberman D A, Cromer D T and Waber J T 1971 *Comput. Phys. Commun.* **2** 107